J. Fac. Pharm. Ankara / Ankara Ecz. Fak. Derg., 49(3): 615-630, 2025
Doi: 10.33483/jfpau.1526137

ORIGINAL ARTICLE / ÖZGÜN MAKALE

DIPEPTIDYL-PEPTIDASE-4 INHIBITORS FROM TINOSPORA CRISPA AS REVEALED BY METABOLOMICS STUDY, MOLECULAR DOCKING AND MOLECULAR DYNAMICS SIMULATION APPROACHES

METABOLOMİ ÇALIŞMALARI, MOLEKÜLER DOKUNMA VE MOLEKÜLER DİNAMİK SİMÜLASYON YAKLAŞIMLARIYLA ORTAYA ÇIKAN TİNOSPORA CRİSPA'DAN DİPEPTİDİL-PEPTİDAZ-4 İNHİBİTÖRLERİ

Andri PRASETIYO[1]*, Shirly KUMALA[1], Esti MUMPUNI[1], Raymond R. TJANDRAWINATA[2], Nancy Dewi YULIANA[3]

[1]Pancasila University, Faculty of Pharmacy, 12640, Jakarta, Indonesia
[2]Atma Jaya Catholic University, Faculty of Biotechnology, 15345, Banten, Indonesia
[3]IPB University, Department of Food Science and Technology, 16680 Bogor, Indonesia

ABSTRACT

Objective: *This study aims to identify potential compounds as inhibitors of DPP-4 from Tinospora crispa.*
Material and Method: *Tinospora crispa stem powder was extracted by ultrasonication. The DPP-4 inhibition test used the MAK 203 screening kit protocol. LC-MS/MS was used to determine the chemical profile. MetaboAnalyst5 and SIMCA were used to analyze the dataset. Molecular docking was performed using Molegro virtual docker, and molecular dynamics simulations were performed using YASARA dynamics employing the AMBER14 force field.*
Result and Discussion: *The percentage inhibition of DPP-4 results showed that the most active was 96% ethanol extract. Orthogonal projection to latent structure (OPLS) analysis provides that 6'-O-LactoylBorapetoside B correlates most with DPP-4 inhibitory activity based on VIP value and Y coefficient. In the docking molecular analysis, 6'-O-LactoylBorapetoside B was predicted to be active as DPP-4 inhibitors with a lower rerank score (−106.51 Kcal/Mol) than alogliptin as a reference (−96.02 Kcal/mol). In molecular dynamics simulation for 100 ns, 6'-O-LactoylBorapetoside B complex of binding with DPP-4 protein was stable with the movement of the RMSD value below 3Å. 6'-O-Lactoyl Borapetoside B has a potential of being a DPP-4-inhibitor. But these results must be tested in vitro and in vivo in order to confirm its activity as a DPP-4 inhibitor.*
Keywords: *6'-O-LactoylBorapetoside B, computer-assisted drug discovery, DPP-4, Tinospora crispa*

ÖZ

Amaç: *Bu çalışmanın amacı, Tinospora Crispa'dan DPP 4'ün inhibitörleri olarak potansiyel bileşikleri tanımlamaktır.*
Gereç ve Yöntem: *Tinospora crispa sapının tozu ultrasonikasyonla ekstrakte edildi. DPP-4 inhibisyon testinde MAK 203 tarama kiti protokolü kullanıldı. Kimyasal profilin belirlenmesinde*

* **Corresponding Author / Sorumlu Yazar:** Andri Prasetiyo
e-mail / e-posta: andriprasetiyo@univpancasila.ac.id, **Phone / Tel.:** +62217864728

Submitted / Gönderilme : 08.08.2024
Accepted / Kabul : 09.04.2025
Published / Yayınlanma : 19.09.2025

LC-MS/MS kullanıldı. Veri setinin analizinde MetaboAnalyst5 ve SIMCA kullanıldı. AMBER14 kuvvet alanını kullanan YASARA dinamikleri kullanılarak moleküler dinamik simülasyonları yapıldı.

Sonuç ve Tartışma: *DPP-4'ün yüzde inhibisyonu sonuçları en aktif olanın %96 etanol ekstraktı olduğunu gösterdi. Latent yapıya dik projeksiyon (OPLS) analizi, 6′-O-LactoylBorapetoside B'nin, VIP değeri ve Y katsayısına dayalı olarak DPP-4 inhibitör aktivitesi ile en fazla korele olduğunu sağlar. Yerleştirme moleküler analizinde, 6′-O-LactoylBorapetoside B'nin, referans olarak alogliptin'den (−96.02 Kcal/mol) daha düşük bir yeniden sıralama skoru (−106.51 Kcal/Mol) ile DPP-4 inhibitörleri olarak aktif olduğu tahmin edildi. 100 ns'lik moleküler dinamik simülasyonunda, 6′-O-LactoylBorapetoside B kompleksinin DPP-4 proteini ile bağlanma kompleksi, RMSD değerinin 3Å'un altındaki hareketi ile stabildi. 6′-O-Lactoyl Borapetoside B, bir DPP-4 inhibitörü olma potansiyeline sahiptir. Ancak bu sonuçların, bir DPP-4 inhibitörü olarak aktivitesini doğrulamak için in vitro ve in vivo olarak test edilmesi gerekir.*

Anahtar Kelimeler: *6′-O-LactoilBorapetosit B, bilgisayar destekli ilaç keşfi, DPP-4, Tinospora crispa*

INTRODUCTION

Diabetes mellitus is a metabolic disease. Defects cause diabetes in insulin secretion, or the insulin does not work optimally, or because of both [1]. Patients with this disease are at high risk for long-term macro- and microvascular complications due to its chronic metabolic imbalance. If they do not receive high-quality care, this puts the patients at risk for complications such as frequent hospitalization and an increased risk of cardiovascular diseases [2]. More than one in ten persons worldwide today have diabetes. A growing number of nations have adult populations where diabetes affects one in five or even more people. The projected prevalence of diabetes in adults aged from 20 to 79 has more than tripled since the first edition in 2000, which rises from an estimated 151 million (4.6%) of the world' population at the time to 537 million (10.5%) today. By 2030, 643 million individuals, or 11.3% of the world's population, will have diabetes, based on our forecast. If the current trends hold, the figure will increase to an astounding 783 million (12.2%) by 2045 [1].

Dipeptidyl Peptidase-4 (DPP-4) is a serine protease enzyme that cleaves peptides on amino acids 2 and 3 of the N-terminal, especially when the amino acid is alanine or proline [3]. The incretin hormone glucagon-like peptide 1 (GLP-1) is a substrate for DPP-4. DPP-4 will cleave amino acid alanine at number 2 GLP-1, so GLPI-1 is not active. GLP-1 lowers blood glucose by increasing insulin secretion and inhibiting glucagon secretion [4]. DPP-4 inhibitors have a mechanism of action in reducing blood glucose in type 2 diabetes patients by inhibiting DPP-4 [5]. The inhibition of DPP-4 prevents the inactivation of the incretin hormone GLP-1.

Hypoglycemic conditions should be avoided in older adult diabetic patients [6]. The combination of metformin and dipeptidyl-peptidase-4 (DPP-4) inhibitors can control blood glucose levels without increasing the risk of hypoglycemia [7,8]. In all the patients with diabetes mellitus, DPP-4 inhibitors are efficient and well-tolerated. These do not raise the risk of CV disease, weight gain, or excessive hypoglycemia [9]. DPP-4 inhibitors also reduce the risk of hypoglycemia, So it may be the drug of choice in adults and older patients [6,10,11]. However, the cost of treating diabetes with DPP-4 inhibitors is much higher than that of the cost of other antidiabetic drugs [12]. Therefore, alternative natural medicines are needed

Tinospora crispa is a medicinal plant of the genus Tinospora from the family Menispermaceae, which is widely distributed in Southeast Asia, especially in Thailand, Malaysia, the Philippines, Indonesia, and the northeastern region of India [13]. *Tinospora crispa* has long been used as a traditional antidiabetic drug. *Tinospora crispa* is known as Brotowali and has been used traditionally in treating several diseases, like diabetes, in Indonesia [14]. The ethanol extract *Tinospora crispa* was shown to be a DPP-4 inhibitor in vitro at a concentration of 2.5 µg/ml with a percentage of inhibition of 65.86 [15]. However, the active compound responsible for the inhibition of DPP-4 is not yet known. *Tinospora crispa* contains a lot of secondary metabolites. The main biologically active compounds of *Tinospora crispa* are terpenoids and terpenoid glycosides. Most terpenoid glycosides are Borapetoside A-F [16,17]. Furthermore, *Tinospora crispa* contains diterpenoids as main components and is predicted to be an

active compound [18]. The use of computational techniques has reduced the time and expense needed for the drug design and discovery process. Molecular docking is one of these techniques used to clarify the binding mechanism for therapeutic candidate molecules The stability level of the resultant target-compound complexes derived from the docking is then assessed using molecular dynamics (MD) simulation [6].

The novelty of this study is identifying bioactive compounds from the stem of *Tinospora crispa* as inhibitors of DPP-4 by using a metabolomic study. The laborious repeated chromatographic separation required in identifying active compounds was eliminated by metabolomics research. In this research, we identified compounds acting as DPP-4 inhibitors and evaluated their molecular activities using a metabolomics study, molecular docking, and dynamic simulation. The goal of molecular dynamics simulation is to see the stability of the protein-ligand complex from the best molecular docking results. The compounds contained in *Tinospora crispa* were obtained by using the metabolomics approach.

MATERIAL AND METHOD

Materials

Tinospora crispa was obtained from the Tawangmangu plantation, Central Java, Indonesia. Plant determination was performed at the Center for Research and Development of Traditional Medicinal, and Medicinal Plants (B2P2TOOT), the Ministry of Health of the Republic of Indonesia. The specimen vouchers were stored at the Faculty of Pharmacy, University Pancasila. Acetonitrile, analytical grade methanol, DPP-4 screening kit, and sitaglipin (MAK 2023) were purchased from Sigma-Aldrich (Sigma-Aldrich Gmbh, Sternheim, German).

Extraction

Ten grams of *Tinospora crispa* stem powder was extracted by ultrasonication for 60 minutes at 40 °C with various solvents such as 96% ethanol, 50% ethanol, and pure water. The ratio of *Tinospora crispa* powder and the extracting solvent volume was 1:10. Extraction was done three times. The solvent evaporated until thick using a rotary evaporator temperature of 40°C.

DPP-4 Inhibition Activity Assay

The DPP-4 inhibition test used the MAK 203 screening kit protocol. The sitaglipin was used as a positive control. Forty-nine microliters of buffer solution, 1 µl of DPP IV enzyme, and 25 µl of sample solution (100 ppm) were put into the well, shaken, and then incubated for 10 minutes at 37°C. Then, 23 µl of buffer solution and 2 µl of the substrate were added and shaken. In the control wells, the inhibitor was replaced with a buffer. Then, it was measured at an excitation wavelength of 360 nm and an emission wavelength of 460 nm using a microplate reader [19].

% Relative Inhibition

$$\text{Slope} = \frac{(\text{FLU2}-\text{FLU1})}{(\text{T2}-\text{T1})} = \Delta\text{FLU/minute} \quad (1)$$

$$\%\ \text{Relative Inhibition} = \frac{(\text{Slope}_{\text{EC}} - \text{Slope}_{\text{SM}})}{\text{Slope}_{\text{EC}}} \times 100\% \quad (2)$$

where: slope_{SM} = the slope of the Sample Inhibitor, slope_{EC} = the slope of the enzyme control

Data were analyzed using Tukey's Honest Significant Difference (HSD) test to determine the statistical significance of differences between treatment groups.

Metabolomic Study with LC-MS/MS

Ultra-high–performance liquid chromatography (UHPLC) 1290 Infinity II HPLC System (Agilent, UK) with a binary pump and an autosampler was used for HPLC analysis. The samples were separated using a Zorbax XDB C18 column (150 mm 4.6 mm i.d., 3.5 µm, Agilent Technologies,

Germany) at room temperature. The samples were separated using a Zorbax XDB C18 column (3.5 µm, 150 × 0.5 mm, Agilent Technologies, Germany). Acetonitrile (B) and 0.1% (v/v) formic acid in water (A) made up the mobile phase, and the elution gradient was configured as follows: 0–1.82 min, 8–12% B; 1.82–10.22 min, 12–16% B; 10.22–18.62 min, 16–25% B; 18.62–31.22 min, 25–46% B; 31.22–33.32 min, 46–58% B; 33.32–39.62 min, 58–65% B; 39.62–43.82 min, 65–68% B. A flow rate of 1.4 ml/min was used.[1] Tandem 6545 QTOF (Agilent, UK) mass spectrometer was linked to the HPLC system by using a dual AJS-ESI interface. Negative ion mode complete scan data was gathered from m/z 250 to 1000. The data collection and analysis were performed on a mass Hunter qualitative analysis.

ProteoWizard was used in converting first raw LC-MS spectra from vendor format to mzML and centroid them [20]. An automated pipeline with a built-in parameter optimization processes, as described in MetaboAnalys5, was used in processing all centroided spectra [21]. According to the database, manual corrections were made to the remaining unclear compounds and peaks. All the compounds were found to have exact mass errors within 5 ppm [22]. The mass error was calculated by.

$$\text{ppm error} = \frac{\text{Theoretical } \frac{m}{z} \text{ value} - \text{Observed } \frac{m}{z} \text{ value}}{\text{Theoretical } \frac{m}{z} \text{ value}} \times 10^6 \quad (3)$$

By using the appropriate functions in MetaboAnalyst5, a chemometrics analysis (PCA) was performed based on the normalized peak tables. Large datasets are reduced in dimension by a vector space transform in PCA. A data matrix with N observations (rows) and X variables is the foundation for PCA (columns). PCA visualizes the data by converting a multivariate data table into a low-dimensional plane. A score plot was used to show the reduction of spectral variation into a set of principal components (PC), each representing connected spectral differences, new PC variables, and orthogonal to one another. The significant correlation's confidence interval was established at 0.95. Simca-P was used in creating the OPLS model, and the primary active ingredients for DPP-4 inhibition were identified by examining the VIP and regression coefficients. The resulting datasets were transferred to the SIMCA-P software version 17.0 (Umetrics, Umea, Sweden) in order to perform the OPLS. Both the models' data were mean-centered and Pareto-scaled before undertaking these multivariate data analyses. OPLS was applied to flatten the dataset, improve class separation, and identify possible biomarkers. R2Ycum (goodness of fit) and cumulated Q2 were used in order to validate the models' quality (Q2cum, goodness of prediction). In classifying models as having strong (Q2cum 0.5) or poor (Q2cum 0.5) prediction skills, a threshold of 0.5 is commonly used. We used the permutation test to validate the OPLS model and decrease the possibility of overfitting and false-positive results. The plots show the correlation coefficients of the original Y and the permuted Y against the cumulative two R2Ys. The model was deemed accurate if both the regression line's intercepts on the y-axis were negative and all Q2 values from the permuted dataset to the left were lower than the Q2 value on the actual dataset to the right [23]. Subsequently, supervised studies were used to identify variable importance in projection (VIP) values. VIP is a readout of the model's contribution from each x-axis variable. It is totaled over all components and weighted to the Y represented by each element. Thus, VIP ranking indicates the role played by metabolites in the model. In broadening our selection in this investigation, we chose primary metabolites with VIP >0.75. The coefficient plot shows a clear, understandable illustration of the relationships between the X- and Y-variables. The figure shows how the factors in the input affect the outcome.

Molecular Docking

The DPP-4 inhibitory enzyme with code 3G0B was obtained from the protein data bank at RCSB website [24-26]. The crystal structure csomprises the four chains (A, B, C, and D) from which chain A is selected. The water molecules were removed using Molegro virtual docker. We downloaded the structure of the compound which resulted from the metabolomic analysis from PubChem, and then its energy was minimized using the ChemDraw 3D 16 program.

Eight compounds that were identified from the metabolomics LC-MS/MS and sitagliptin as the standard were docked with the DPP-4 with PDB Code 3G0B using Molegro virtual docker. The docking protocol uses a protocol which has been validated in the previous studies [27]. which was the binding site X: 42.21Å, Y: 34.47Å, and Z: 14.97Å, radius 10Å, MolDock Optimizer algorithm (differential

evolution) and Moldock Score scoring function. We compared our result analysis according to the lowest rerank score with alogliptin as the reference.

Molecular Dynamic Simulation

Scene mode in YASARA structure was constructed using the default mode after the best pose of the hit in the virtual screening, which utilizes the Molegro virtual docker, was chosen. Molecular dynamics simulations were performed using YASARA dynamics employing the AMBER14 force field [28]. The scene mode was then put through MD simulations using the YASARA structure macro for the MD run's default settings [29] except for the length of the MD and the intervals for capturing pictures. This study's MD run lasted 100 ns, and the photographs were taken every 10 ps. Trajectory analysis was performed to measure the root mean square deviations (RMSDs). Complex binding of compounds with DPP-4 inhibitors was considered stable if the overall RMSD did not exceed 3.2Å [30].

RESULT AND DISCUSSION

Percentage of DPP-4 Inhibition of *Tinospora crispa* Result

DPP-4 inhibition tests on ethanol extract (96% and 50%) and *Tinospora crispa* stem water with a concentration of 100 ppm have been performed, and the results show that all extracts have activity as inhibitors of DPP-4. The results showed that 96% of the ethanol extract of *Tinospora crispa* stem had the highest percentage of DPP-4 inhibition compared to 50% of the ethanol extract and aqueous extract (Figure 1). DPP-4 inhibition activity of the three extracts was compared using one-way ANOVA statistical analysis. Results indicated a statistically significant difference in inhibition percentages ($p < 0.05$). Tukey's HSD test (post hoc analysis) showed that the DPP-4 inhibition by 96% ethanol extract was significantly higher (67.9%±2.5%) than that by both 50% ethanol extract ($P < 0.01$) and aqueous-extract ($P < 0.01$: mean inhibition = 44.8%±3.1% and 54.1%±2.8% respectively. The main components of *Tinospora crispa* were diterpenoids which were known to have an antidiabetic activity [31–33]. Borapetoside A, B, C, D, E, and F comprised most of the terpenoid glycosides. Both insulin-dependent and insulin-independent mechanisms mediated borapetoside A's hypoglycemic effects.

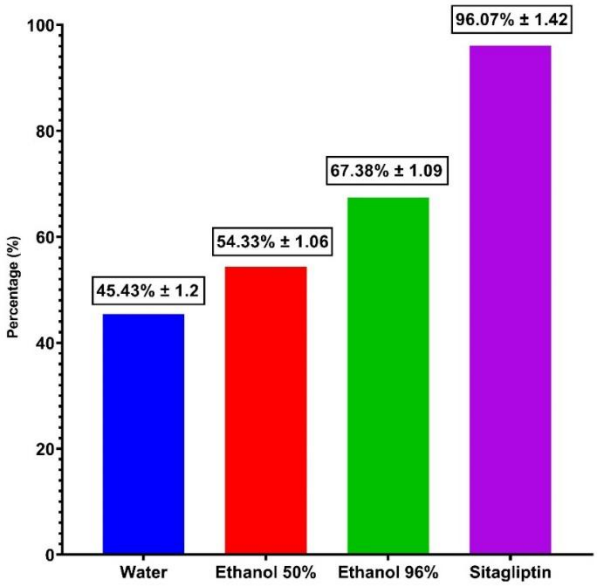

Figure 1. Inhibitory activity of DPP-4 ethanol extract (96% and 50%) and stem water of *Tinospora crispa*

In addition, it was shown that borapetoside A increased glucose consumption in peripheral tissues, decreased hepatic gluconeogenesis, and activated insulin signaling system, which helped in lowering

the plasma glucose levels [34]. Borapetoside C can improve insulin sensitivity, postpone the onset of insulin resistance, and promote glucose utilization. The hypoglycemic effects of Borapetoside C in diabetic mice may be attributed to the stimulation of IR-Akt-GLUT2 expression and the improvement of insulin sensitivity [32]. Diterpenoids are soluble in ethanol but difficult to dissolve in water, so the 96% ethanol extract has the highest percentage of a DPP-4 inhibitor since the diterpenoid content in ethanol extract is 96% which is more than the 50% ethanol extract and water. This observation was consistent with Lam et al [17]. In support of previous studies showing that high-concentration ethanol solvents optimize the extraction ratio of bioactive diterpenoids and elevate the bioactivity in vitro. Additionally, Lam et al. explained that the biological activity of diterpenoids is weak in water-based extractions owing to their low solubility, including DPP-4 inhibition. For this reason, these comparative results further highlight the potential application of tailored solvents to enhance diterpenoid yield and bioactivity.

Metabolomic Study Result

LC-MS/MS was used to conduct metabolomic analysis using the method's recommended configuration parameters. LC-MS/MS analysis presents information on precursor and fragment ions in negative ion mode $[M-H]^-$. The chromatograms obtained from LC-MS/MS were processed by using the MetaboAnalyst5 software. We got the LC-MS/MS chromatogram in a table mass array containing information on normalized peak intensity, retention time, and accurate mass of detected peaks. The complete details on statistically significant secondary metabolites contributing to the inhibition of the DPP-4 enzyme were obtained using multivariate statistical analysis methods. By grouping or splitting data on the score plot, analysis techniques like PCA and OPLS can display the correlation between each class [23]. Then, the data were analyzed by using PCA. PCA analysis (Figure 2) results present that on the score plot, PC1(54.5%) and PC2 (30.8%) explain 85.3% of the total variance in the dataset. The results of the multivariate analysis using the PCA method (Figure 2) indicate the clear separation of sample groups3 based on differences in treatment (differences in solvent). Therefore, the metabolite profiles of the three solvents were different from each other. The group separation of the ethanol extract (96%) was clear as compared to the ethanol extract (50%) and water, which indicated that the metabolite profile of the ethanol extract (96%) was different from that of the other two extracts.

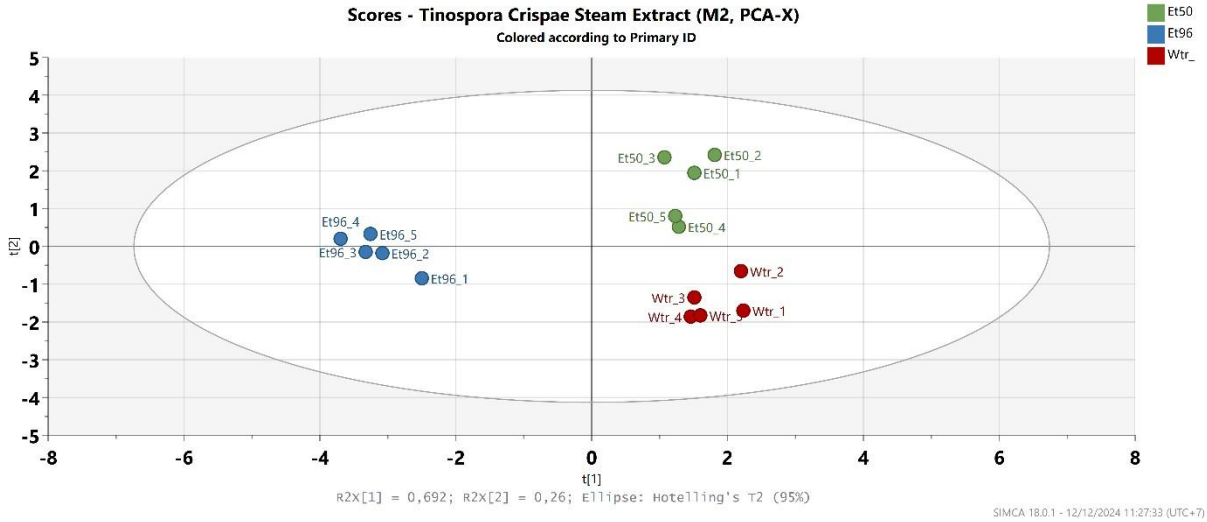

Figure 2. PCA score plots were generated using the Simca from LC-MS data on sample *Tinospora crispa* stem extract metabolites. Different colors indicate different solvents; purple (water), pink (ethanol 50%), and green (ethanol 96%)

According to the fragment pattern and m/z retrieved from METLIN [35], PubChem [36], and other databases, the potential metabolites were searched for and chosen. The compounds were identified from the peaks $[M-H]^-$ at m/z 533.2036, 535.2191, 537.1985, 551.2142, 567.2092, 581.2249, 623.2354,

and 697.2717, respectively. The compounds were Borapetoside F [$C_{27}H_{34}O_{11}$], Borapetoside C [$C_{27}H_{36}O_{11}$], borapetoside A [$C_{26}H_{34}O_{12}$], Borapetoside B[$C_{27}H_{36}O_{12}$], Rumphioside A [$C_{27}H_{36}O_{13}$], Rumphioside B [$C_{28}H_{38}O_{13}$], 6'-O-Lactoyl Borapetoside B[$C_{30}H_{40}O_{14}$], and Borapetoside D [$C_{33}H_{46}O_{16}$]. For detailed data, see Table 1, which lists down the determined molecular formulas, theoretical masses, observed m/z values, mass errors (in parts per million), and hypothesized structures for the eight metabolites found from the *Tinospora crispa* stem extract.

Table 1. Exact mass data from QTOF LC-MS/MS of *Tinospora crispa* stem

No	Mass			Assigned adduct	Formula	Identification
	M/Z Theoretical	M/Z Observed	Error (ppm)			
1	533.2017	533.2036	−3.54	$[M-H]^-$	$C_{27}H_{34}O_{11}$	Borapetoside F
2	535.2174	535.2191	−3.30	$[M-H]^-$	$C_{27}H_{36}O_{11}$	Borapetoside C
3	537.1967	537.1985	−3.50	$[M-H]^-$	$C_{26}H_{34}O_{12}$	Borapetoside A
4	551.2123	551.2142	−3.45	$[M-H]^-$	$C_{27}H_{36}O_{12}$	Borapetoside B
5	567.2072	567.2092	−3.49	$[M-H]^-$	$C_{27}H_{36}O_{13}$	Rumphioside A
6	581.2229	581.2249	−3.51	$[M-H]^-$	$C_{28}H_{38}O_{13}$	Rumphioside B
7	623.2334	623.2354	−3.17	$[M-H]^-$	$C_{30}H_{40}O_{14}$	6'-O-LactoylBorapetoside B
8	697.2702	697.2717	−2.13	$[M-H]^-$	$C_{33}H_{46}O_{16}$	Borapetoside D

The results of the OPLS score plot from the LC-MS data indicate that there has been a grouping of samples based on their activities (Figure 3). The model which correlated well with the inhibitory activity of the DPP-4 enzyme was the 96% ethanol extract of *Tinospora crispa*, located on the upper right of the X-ordinate axis. In comparison, the ethanol extract of 50% of *Tinospora crispa* was located in the middle of the X-ordinate axis, and the aqueous extract of *Tinospora crispa* had the least activity. It was located on the top left X-ordinate axis. As can be gleaned from this, it can be concluded that the OPLS model can completely separate samples based on their activities.

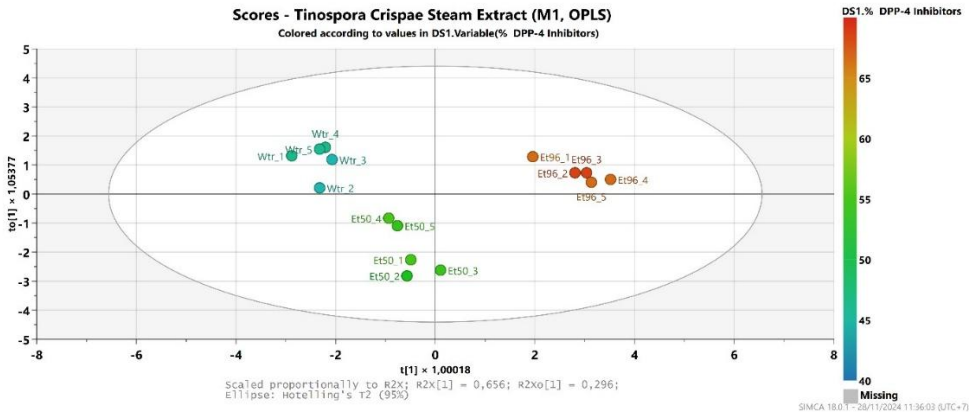

Figure 3. *Tinospora crispa* extracts in a scatter plot of LC-MS OPLS scores. The values which followed stood for extraction solvents (Et96 = ethanol 96%, Et50 = ethanol 50%, and Wtr = water, respectively) and replication. Lower to higher values are represented by the colors blue and red

We have validated the OPLS model by evaluating its quality with cross-validation ANOVA (CV-ANOVA) and permutation methods (as can be shown in Figure 3). CV-ANOVA has been performed by calculating the *p*-value to estimate the validity of the OPLS model. The requirement for the *p*-value of CV-ANOVA is below 0.05 [37]. The goal of validating the OPLS model with a permutation test is to avoid false findings and reduce the risk of overfitting. The permutation test was performed by developing a new model in which the data on the inhibition of the DPP-4 enzyme was reordered randomly. R2Y and Q2Y values of the new model were compared to the original model [23]. The permutation test results obtained two values, R2 (goodness of fit) and Q2 (excellence of prediction). If all the R2Y and Q2Y scores of the new model must be lower than that of the original model or minimize the overlap between the two groups, then the model is considered to be valid. If the $Q2 \geq 0.5$, the OPLS model has a good predictive ability [38]. The results of the OPLS LC-MS validation were considered valid since the *p*-value of CS-ANOVA is 1.06364×10^{-5}, and the Q2 value of the permutation test (Figure 4) was 0.583, R2Y and Q2Y of the new model which was consistently lower than that of the original.

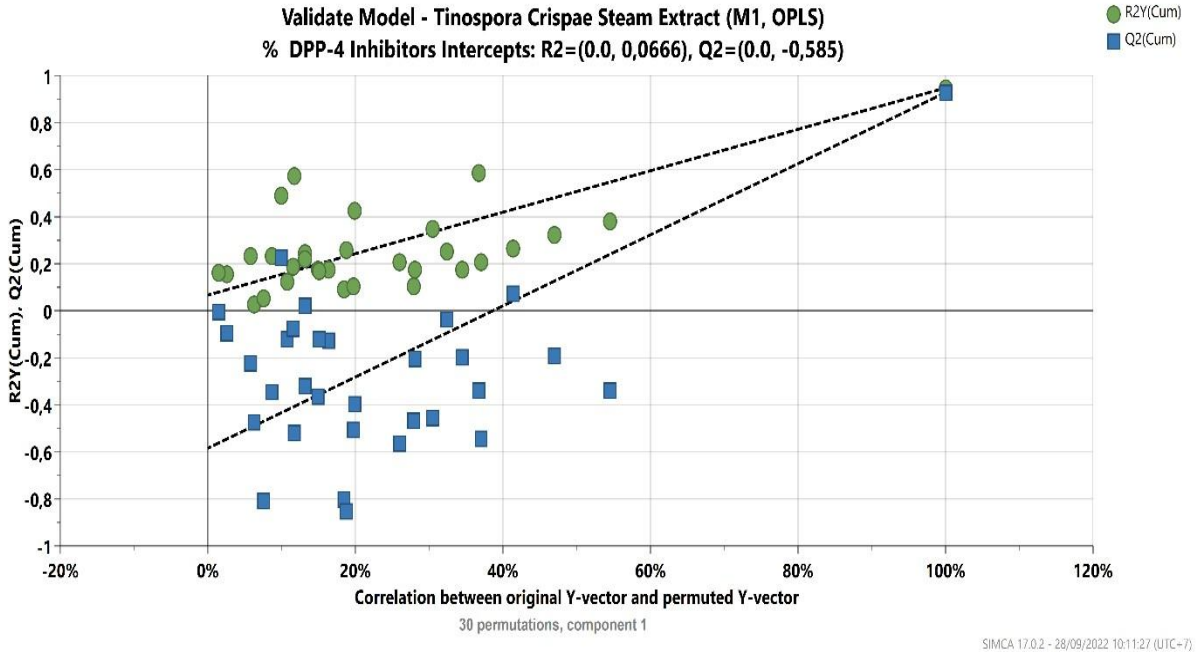

Figure 4. Permutation test model graphs for OPLS scores. 30 randomly selected permutations were used for the permutation tests

The loading plot of the variable importance projection (VIP) model shows the contribution of each X variable to the projection. VIP scores indicate that the X variable plays a vital role in explaining the variation in Y. The VIP score in this study was used to assess the contribution of compounds from *Tinospora crispa* to inhibitors of the DPP-4 enzyme. We use the VIP score ≥ 0.75 as the criterion for the variable choice [39]. The VIP score results (Figure 5) presented five compounds that have a VIP score of ≥0.75 such as Borapetoside C, 6'-O-LactoylBorapetoside B, Rumphioside A, Borapetoside D, and Rumphioside B, Borapetoside B, Borapetoside F, and borapetoside A. These compounds significantly affected the effect on the percentage of DPP-4 enzyme inhibition, but the VIP score could not determine whether the impact was positive or negative on the DPP-4 enzyme inhibition. Thus, we have analyzed it further by using the coefficient score analysis.

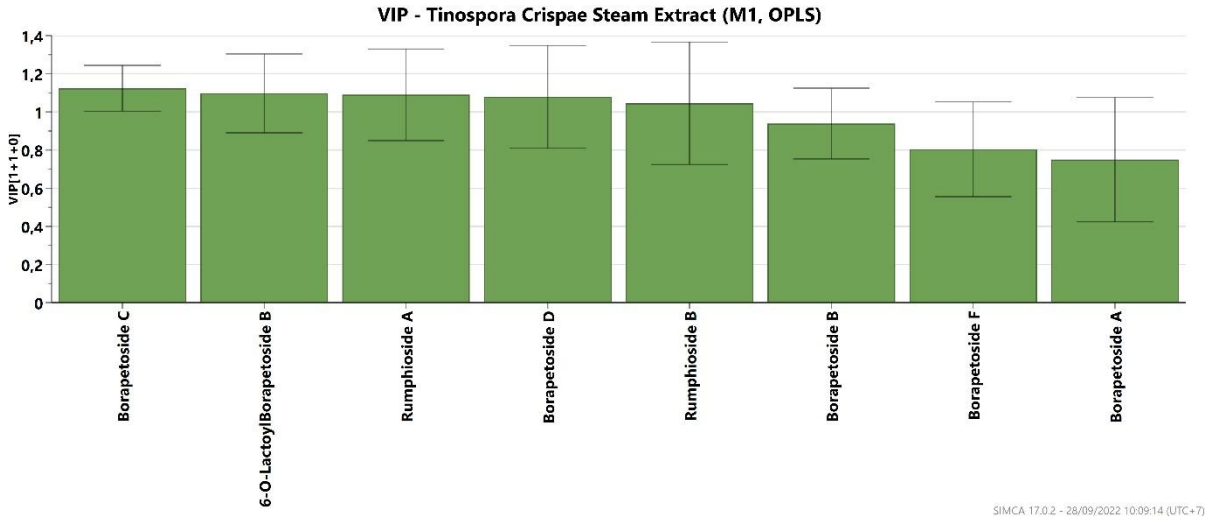

Figure 5. Results of the OPLS analysis which used the VIP plot indicating the importance of each variable in relation to the predictive component

A positive coefficient value indicates that the compound has an activity as an inhibitor of the DPP-4 enzyme. In contrast, a negative coefficient value indicates that the compound has no activity as an inhibitor of the DPP-4 enzyme. The results of the score coefficient analysis (Figure 6) provide that 6'-O-LactoylBorapetoside B, Borapetoside C, Rumphioside B, and Borapetoside D have an activity as an inhibitor of the DPP-4 enzyme since they had a positive coefficient score. Base on the score coefficient, 6'-O-LactoylBorapetoside has the best activity as a DPP-4 inhibitor. Borapetoside A, Borapetoside F, and Borapetoside B did not have activity as inhibitors of the DPP-4 enzyme since they all had negative coefficient scores.

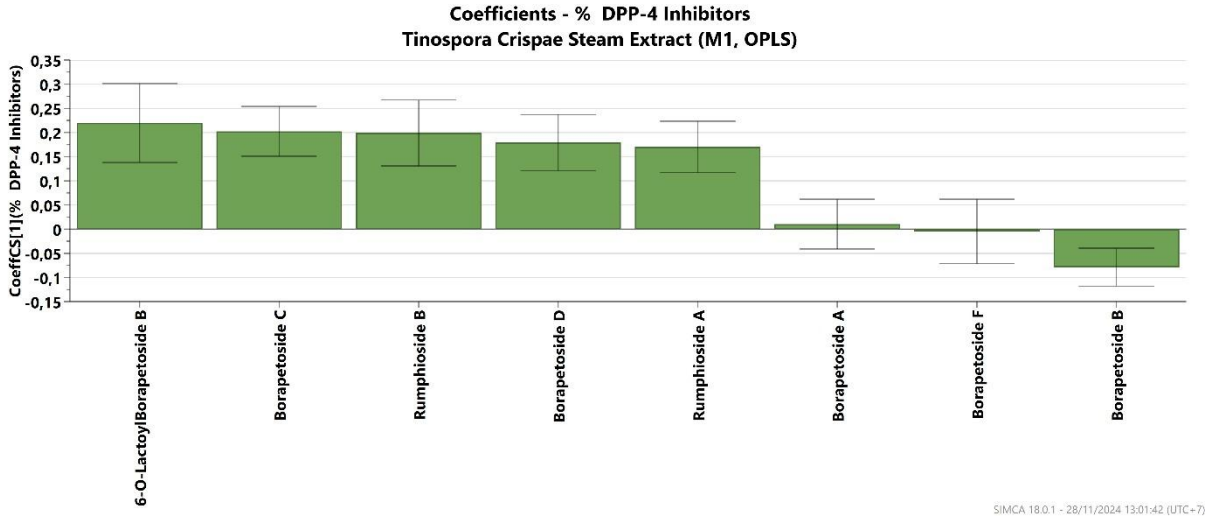

Figure 6. Profile coefficient for Y plot in identifying the substances which cause the samples to separate in the score scatter plot

Molecular Docking Simulation Result

The compounds from the stem extract of *Tinospora crispa*, which were predicted to have positing correlations as inhibitors of DPP-4 from the results of the metabolomic study, were confirmed by

molecular docking simulation. Docking validation ensures that the native ligand can re-occur with the binding site—docking validation success parameters based on the results of the root mean square deviation (RMSD) value. We used the criteria RMSD value of less than 1Å as a parameter for validation success [40]. The results of the redocking validation obtained an RMSD value of 0.5844Å, which indicates that the validation has met the excellent criteria since the RMSD value is below 1Å. Figure 7A presents the native ligand pose after docking (yellow) occupying the binding site accurately with the native ligand pose before docking (red). The bound ligand interacts with the structure very well. The ligand interacts with the structure with six hydrogen bonds Glu205, Glu206, Tyr547, Tyr631, Tyr662, Asn710 with the enzyme (Figure 7B). Similar hydrogen bonding locations were found in the prior experimental investigation. The quantity of hydrogen bonds in this investigation and those reported by the experimental study were comparable [24]. Therefore, it was discovered that the results of this study's docking of the bound ligand to the crystal structure were comparable to those of earlier experiments.

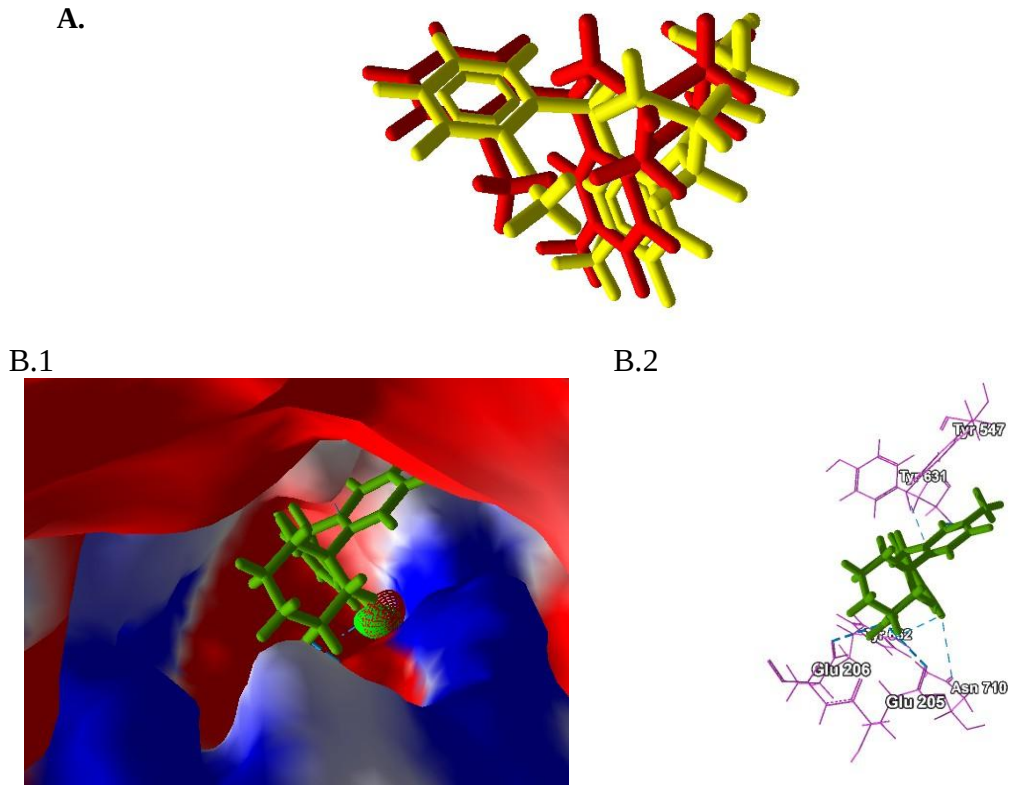

Figure 7. A) Redocking validation, native ligand (yellow) after docking and native ligand (red) before docking, B) Binding mode of DPP-4 inhibitor, B.1 its binding pose in the binding site, B.2 its 3D binding

The results of the molecular docking simulation of the five compounds (see Table 2) which are positively correlated as DPP-4 inhibitors show a rerank score of 6'-O-Lactoyl Borapetoside B, Borapetoside C, Rumphioside B, and Borapetoside D (−97.43 to −111.43 Kcal/mol) lower than alogliptin as reference (−96.02 Kcal/mol). Additionally, the hydrogen bond interaction analysis of amino acid residues showed that Rumphioside B and 6'-O-LactoylBorapetoside had hydrogen bonds Glu205 and Glu206, where the amino acid residues Glu205 and Glu206 had a vital role in inhibiting the DPP-4 enzyme [41]. However, 6'-O-Lactoyl Borapetoside B was predicted to have a better DPP-4 inhibitory activity than Rumphioside B since 6'-O-LactoylBorapetoside B, besides having amino acid residues Glu205 and Glu206 also has Ser630. However, 6'-O-Lactoyl Borapetoside B is predicted to have a better

DPP-4 inhibitory activity than Rumphioside B since 6'-O-Lactoyl Borapetoside B, besides having amino acid residues Glu205 and Glu206, also has Ser630. The amino acid residue Ser630 is one of the Triad catalytic enzymes which can increase its ability as a DPP-4 inhibitor. These molecular docking simulation results also confirm the metabolomics study's findings. Molecular dynamics simulations further confirmed the molecular docking simulation results, ensuring that the 6'-O-LactoylBorapetoside B complex bond with the DPP-4 enzyme was stable.

Table 2. Rank score and hydrogen bonds of amino acid residues (kcal/mol) of the five compounds obtained from OPLS

Number	Compounds	Rerank score (Kcal/mol)	Hydrogen bonding interactions of amino acid residues
1	Alogliptin (Reference)	−96.02	Glu205, Glu206, Tyr547, Tyr631, Tyr662, Asn710
2	Rumphioside B	−111.44	Glu205, Arg669, Glu206, Tyr662, Tyr547, Tyr666, Ser209
3	Borapetoside D	−107.09	Glu205, Tyr631, Gly632, Tyr662
4	6'-O-LactoylBorapetoside B	−106.51	Glu205, Glu206, Ser630, Arg125
5	Rumphioside A	−100.63	Glu206, Tyr547, Tyr666, His126, Ser209
6	Borapetoside C	−97.43	Glu206, Tyr547, Tyr666, His126, Ser209

Molecular Dynamic Simulation Result

The stability of the protein structure upon ligand binding and the system's equilibrium process is monitored by the radius of gyration and RMSD of the protein structure as a function of time [42]. The radius of gyration analysis (Rg) for the MD simulation indicates the compactness of the protein structure. Rg was computed here to analyze the structural stability of DPP-4 protein bound with test ligand during 100 ns simulation. The Rg plot (Figure 8) displayed an average value ranging between 26.5–27.6 Å, verifying the protein structure stabilized itself without drastic changes in compactness during the simulation. Small changes in Rg values (<0.5 Å) indicate the stable interaction of the protein with the ligand, and suggest no unfolding of the protein by the ligand. The RMSD of Cα atoms To examine the structural stability of the DPP-4 protein during the molecular dynamics (MD) simulation in YASARA, the root mean square deviation (RMSD) of the C-alpha atoms was analyzed. C alpha RMSD simulation results for 100 ns (Figure 9), we found that the protein-ligand complex experienced equilibrium after the first 10 ns, while the RMSD value was between 1.6–2.6 Å. Such a narrow range indicates that there is little perturbation of the initial conformation and thus validates the stability of the system during the short simulation time. Cα RMSD results as well, are consistent with other stability indicators, including radius of gyration (Rg), which characterizes the compactness and maintenance quality of the protein-ligand complex structure. The RMSD ligan movement (in Figure 10) is used in MD simulation to evaluate structural departure from the starting protein structure [42]. The stability of the enzyme-inhibitor interaction was investigated next using molecular dynamics simulations by utilizing the optimal pose of 6'-O-Lactoyl Borapetoside B in 3G0B obtained from the prior molecular docking studies as the beginning point. As can be seen from Figure 8, a rise in the RMSD values of the 3G0B's 6'-O-Lactoyl Borapetoside B was seen throughout 1–100 ns. In the production run of the MD simulations, the 6'-O-Lactoyl Borapetoside B RMSD values ranged from 2.068 to 2.539Å. The RMSD's average deviation was 0.223, and its standard deviation was 0.070. The poses of 6'-O-Lactoyl Borapetoside B remained steady during the MD's production run, as indicated by the RMSD values below 3.2Å during equilibrium processes. The maximum value of RMSD is 3.2Å [43], which indicates a better docking position, and the enzyme structure is not disturbed. The results of molecular dynamic simulations have confirmed the findings from metabolomic studies and molecular docking simulations that 6'-O-Lactoyl Borapetoside B has a great potential activity as a DPP-4 inhibitor.

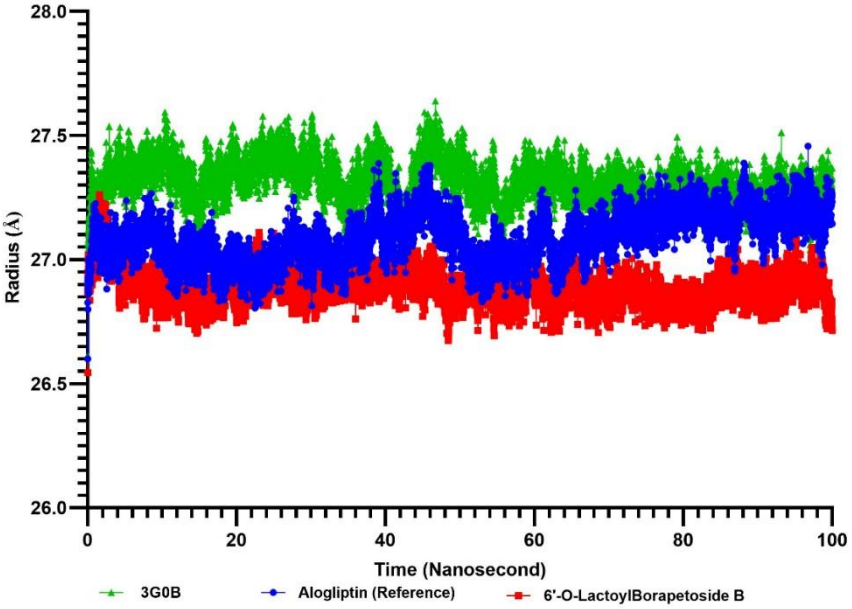

Figure 8. The radius of gyration for the ligand atoms in relation to each complex's initial structure and simulation time

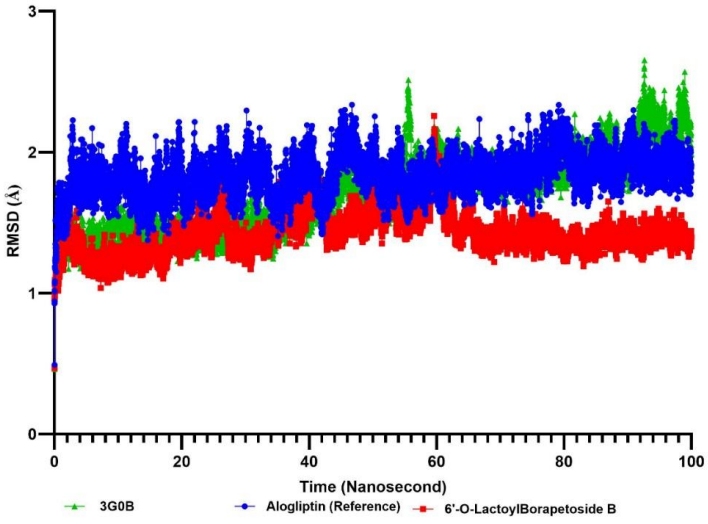

Figure 9. The RMSD Cα for the ligand atoms in relation to each complex's initial structure and simulation time

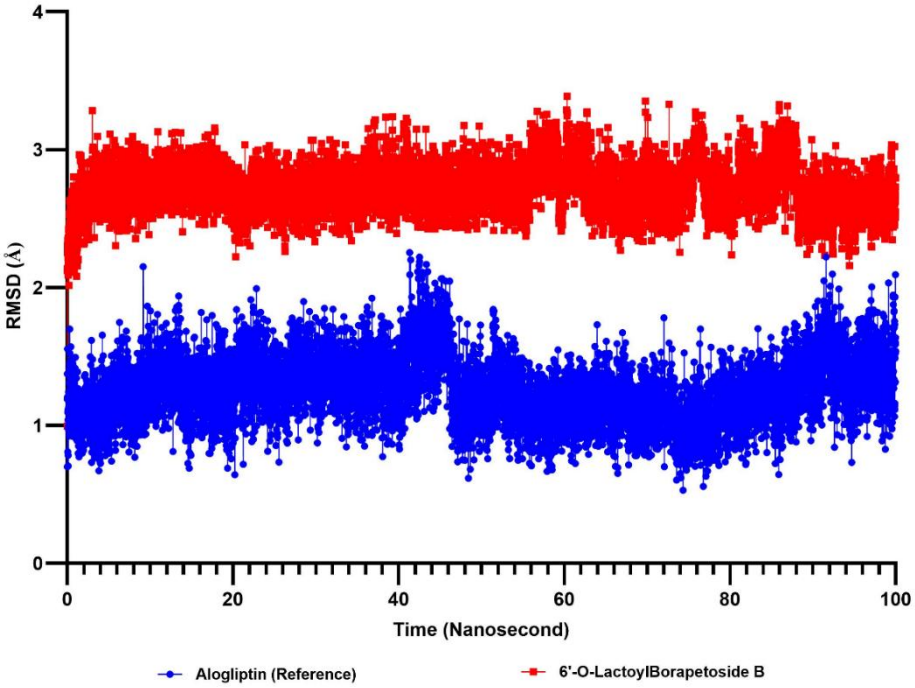

Figure 10. The RMSD for the ligand atoms in relation to each complex's initial structure and simulation time

The compound 6'-O-LactoylBorapetoside B has been identified which has excellent potential as an inhibitor of DPP-4 from *Tinospora crispa* stems from a metabolomic study approach based on LC-MS/ms, molecular docking, and molecular dynamic simulation. Information on these compounds can be used as a quality control marker.

ACKNOWLEDGEMENTS

The author would like to thank Prof. Dr. Siswandono, Apt, Department of Pharmaceuticals Chemistry, Airlangga University, for permission and support in software facilities Molegro virtual docker.

AUTHOR CONTRIBUTIONS

Concept: A.P., R.R.T.; Design: A.P., S.K.; Sources: A.P., S.K., E.M., R.R.T., N.D.Y.; Materials: S.K., E.M.; Data Collection and/or Processing: A.P., N.D.Y.; Analysis and/or Interpretation: S.K., E.M., R.R.T.; Manuscript Writing: A.P., S.K.; Critical Review: E.M., R.R.T., N.D.Y.; Other: -

CONFLICT OF INTEREST

The authors declare that there is no real, potential, or perceived conflict of interest for this article.

ETHICS COMMITTEE APPROVAL

The authors declare that the ethics committee approval is not required for this study.

REFERENCES

1. International Diabetes Federation. (2021). International Diabetes Federation. In E.J. Boyko, D.J. Magliano, S. Karuranga, L. Piemonte, P. Riley, P. Saeedi and S. Hong (Eds.), IDF Diabetes Atlas, 10th edition. Ireland: Elsevier. [CrossRef]

2. Chaudhury, A., Duvoor, C., Reddy Dendi, V.S., Kraleti, S., Chada, A., Ravilla, R., Marco, A., Shekhawat, N.S., Montales, M.T., Kuriakose, K., Sasapu, A., Beebe, A., Patil, N., Musham, C.K., Lohani, G.P., Mirza, W. (2017). Clinical review of antidiabetic drugs: implications for type 2 diabetes mellitus management. Frontiers in Endocrinology, 8(6), 1-12. [CrossRef]
3. Nauck, M.A., Meier, J.J. (2018). Incretin hormones: Their role in health and disease. Diabetes, Obesity and Metabolism, 20, 5-21. [CrossRef]
4. Nauck, M. (2016). Incretin therapies: Highlighting common features and differences in the modes of action of glucagon-like peptide-1 receptor agonists and dipeptidyl peptidase-4 inhibitors. Diabetes, Obesity and Metabolism, 18(3), 203-216. [CrossRef]
5. Omar, B., Ahrén, B. (2014). Pleiotropic mechanisms for the glucose-lowering action of DPP-4 inhibitors. Diabetes, 63(7), 2196-2202. [CrossRef]
6. Muhammed, M.T., Aksoy, N., Kirilmaz, A., Türkmen, E. (2024). Towards understanding natural alpha-glucosidase inhibitors: A computational study. Journal of Faculty of Pharmacy of Ankara University, 48(1), 205-14. [CrossRef]
7. Gooßen, K., Gräber, S. (2012). Longer term safety of dipeptidyl peptidase-4 inhibitors in patients with type 2 diabetes mellitus: systematic review and meta-analysis. Diabetes, Obesity and Metabolism, 14(12), 1061-1072. [CrossRef]
8. Karagiannis, T., Paschos, P., Paletas, K., Matthews, D.R., Tsapas, A. (2012). Dipeptidyl peptidase-4 inhibitors for treatment of type 2 diabetes mellitus in the clinical setting: Systematic review and meta-analysis. BMJ (Online), 344, 1-15. [CrossRef]
9. Deacon, C.F. (2018). A review of dipeptidyl peptidase-4 inhibitors. Hot topics from randomized controlled trials. Diabetes, Obesity and Metabolism, 20, 34-46. [CrossRef]
10. Buse, J.B., Wexler, D.J., Tsapas, A., Rossing, P., Mingrone, G., Mathieu, C., D'alessio, D.A., Davies, M.J. (2020). 2019 Update to: Management of hyperglycemia in type 2 diabetes, 2018. A consensus report by the American Diabetes Association (ADA) and the European Association for the Study of Diabetes (EASD). Diabetes Care, 43(7), 1-7. [CrossRef]
11. McGuire, H., Longson, D., Adler, A., Farmer, A., Lewin, I. (2016). Management of type 2 diabetes in adults: Summary of updated NICE guidance. BMJ (Online), 353, 1-3. [CrossRef]
12. Geng, J., Yu, H., Mao, Y., Zhang, P., Chen, Y. (2015). Cost effectiveness of Dipeptidyl Peptidase-4 Inhibitors for type 2 diabetes. PharmacoEconomics, 33(6), 581-597. [CrossRef]
13. Thomas, A., Rajesh, E.K., Kumar, D.S. (2016). The significance of *Tinospora crispa* in treatment of diabetes mellitus. Phytotherapy Research, 30(3), 357-366. [CrossRef]
14. Ahmad, W., Jantan, I., Bukhari, S.N.A. (2016). *Tinospora crispa* (L.) Hook. F. & Thomson: A review of its ethnobotanical, phytochemical, and pharmacological aspects. Frontiers in Pharmacology, 7, 1-19. [CrossRef]
15. Riyanti, S., Suganda, A.G., Sukandar, E.Y. (2016). Dipeptidyl peptidase-IV inhibitory activity of some Indonesian medicinal plants. Asian Journal of Pharmaceutical and Clinical Research, 9(2), 375-377.
16. Chi, S., She, G., Han, D., Wang, W., Liu, Z., Liu, B. (2016). Genus tinospora: Ethnopharmacology, phytochemistry, and pharmacology. Evidence-Based Complementary and Alternative Medicine, 2016 (1). [CrossRef]
17. Lam, S., Ruan, C., Hsieh, P., Su, M., Lee, S. (2012). Hypoglycemic diterpenoids from *Tinospora crispa*. Journal of Natural Products, 75(2), 153-159. [CrossRef]
18. Xu, L.L., Guo, F.X., Chi, S.S., Wang, Z.J., Jiang, Y.Y., Liu, B., Zhang, J.Y. (2017). Rapid screening and identification of diterpenoids in *Tinospora sinensis* based on high-performance liquid chromatography coupled with linear ion trap-orbitrap mass spectrometry. Molecules, 22(6), 1-17. [CrossRef]
19. Avogaro, A., Dardano, A., de Kreutzenberg, S.V., Del Prato, S. (2015). Dipeptidyl peptidase-4 inhibitors can minimize the hypoglycaemic burden and enhance safety in elderly people with diabetes. Diabetes, Obesity and Metabolism, 17(2), 107-115. [CrossRef]
20. Chambers, M.C., MacLean, B., Burke, R. Amodei D, Ruderman D.L., Neumann, S., Gatto, L., Fischer, B., Pratt, B., Egertson, J., Hoff, K., Kessner, D., Tasman, N., Shulman, N., Frewen, B., Baker, T.A., Brusniak, M.Y., Paulse, C., Creasy, D., Flashner, L., Kani, K., Moulding, C., Seymour, S.L., Nuwaysir, L.M., Lefebvre, B., Kuhlmann, F., Roark, J., Rainer, P., Detlev, S., Hemenway, T., Huhmer, A., Langridge, J., Connolly, B., Chadick, T., Holly, K., Eckels, J., Deutsch, E.W., Moritz, R.L., Katz, J.E., Agus, D.B., MacCoss, M., Tabb, D.L., Mallick, P. (2012). A Cross-platform toolkit for mass spectrometry and proteomicszwane's mining charter lunacy. Nature Biotechnology, 30(10), 1. [CrossRef]
21. Pang, Z., Chong, J., Zhou, G., De Lima Morais, D.A., Chang, L., Barrette, M., Gauthier, C., Jacques, P.É., Li, S., Xia, J. (2021). MetaboAnalyst 5.0: Narrowing the gap between raw spectra and functional insights. Nucleic Acids Research, 49(W1), W388-W396. [CrossRef]

22. Mihaleva,V.V., Vorst, O., Maliepaard, C., Verhoeven, H.A., de Vos, R.C.H., Hall, R.D., van Ham, R.C.H.J. (2008). Accurate mass error correction in liquid chromatography time-of-flight mass spectrometry based metabolomics. Metabolomics, 4, 171-82. [CrossRef]
23. Mahadevan, S., Shah, S.L., Marrie, T.J., Slupsky, C.M. (2008). Analysis of metabolomic data using support vector machines. Analytical Chemistry, 80(19), 7562-7570. [CrossRef]
24. Zhang, Z., Wallace, M.B., Feng, J., Stafford, J.A., Skene, R.J., Shi, L., Lee, B., Aertgeerts, K., Jennings, A., Xu, R., Kassel, D.B., Kaldor, S.W., Navre, M., Webb, D.R., Gwaltney, S.L. (2011). Design and synthesis of pyrimidinone and pyrimidinedione inhibitors of dipeptidyl peptidase IV. Journal of Medicinal Chemistry, 54(2), 510-524. [CrossRef]
25. RSCB Website. (2021). From https://www.rcsb.org/. Accessed date: 13.07.2021.
26. Berman, H.M., Westbrook, J., Feng, Z., Gilliland, G., Bhat, T.N., Wessig, H., Shindyalov, I.N., Bourne, P.E. (2000). The protein data bank. Nucleic Acid Research, 28, 235-242. [CrossRef]
27. Prasetiyo, A., Kumala, S., Mumpuni, E., Tjandrawinata, R.R. (2022). Validation of structural-based virtual screening protocols with the PDB Code 3G0B and prediction of the activity of *Tinospora crispa* compounds as inhibitors of dipeptidyl-peptidase-IV. Research Results in Pharmacology, 8(1), 95-102. [CrossRef]
28. Krieger, E., Vriend, G. (2015). New ways to boost molecular dynamics simulations. Journal of Computational Chemistry, 36(13), 996-1007. [CrossRef]
29. Krieger, E., Ozvoldik, K. (2003). Yasara Biosciences. From http://www.yasara.org/md run. mcr. Accessed date: 13.07.2021.
30. Mahmud, S., Biswas, S., Paul, G.K., Mita, M.A., Afrose, S., Hasan, Md. R., Shimu, Mst. S.S., Uddin, M.A.R., Uddin, Md. S., Zaman, S., Kibria, K.M.K., Khan, Md. A., Bin Emran, T., Saleh, Md. A. (2021). Antiviral peptides against the main protease of SARS-CoV-2: A molecular docking and dynamics study. Arabian Journal of Chemistry, 14(9), 103315.
31. Lokman, F.E., Gu, H.F., Wan Mohamud, W.N., Yusoff, M.M., Chia, K.L., Östenson, C.G. (2013). Antidiabetic effect of oral borapetol B compound, isolated from the plant *Tinospora crispa*, by stimulating insulin release. Evidence-Based Complementary and Alternative Medicine, 2013, Article ID 727602. [CrossRef]
32. Ruan, C.T., Lam, S.H., Chi, T.C., Lee, S.S., Su, M.J. (2012). Borapetoside C from *Tinospora crispa* improves insulin sensitivity in diabetic mice. Phytomedicine, 19(8–9), 719–724. [CrossRef]
33. Xu, Y., Niu, Y., Gao, Y., Wang, F., Qin, W., Lu, Y., Hu, J., Peng, L., Liu, J., Xiong, W. (2017). Borapetoside E, a clerodane diterpenoid extracted from *Tinospora crispa*, improves hyperglycemia and Hyperlipidemia in high-fat-diet-induced type 2 diabetes mice. Journal of Natural Products, 80(8), 2319-2327. [CrossRef]
34. Ruan, C., Lam, S., Lee, S., Su, M. (2013). Hypoglycemic action of borapetoside A from the plant *Tinospora crispa* in mice. International Journal of Phytotherapy and Phytopharmacology, 20(8-9), 667-675. [CrossRef]
35. METLIN Website. (2021). From https://metlin.scripps.edu. Accessed date: 10.09.2021.
36. Kim, S., Chen, J., Cheng, T., Gindulyte, A., He, J., He, S., Li, Q., Shoemaker, B.A., Thessen, P.A., Yu, B., Zaslavsky, L., Zhang, J., Bolton, E. E. (2021). PubChem in 2021: New data content and improved web interfaces. Nucleic Acids Research. 49(D1), D1388-D1395. [CrossRef]
37. Triba, M.N., Le Moyec, L., Amathieu, R., Goossens, C., Bouchemal, N., Nahon, P., Rutledge, D.N., Savarin, P. (2015). PLS/OPLS models in metabolomics: The impact of permutation of dataset rows on the K-fold cross-validation quality parameters. Molecular BioSystems, 11(1), 13-19. [CrossRef]
38. Yang, Y., Wu, Z., Li, S., Yang, M., Xiao, X., Lian, C., Wen, W., He, H., Zeng, J., Wang, J., Zhang, G. (2020). Targeted blood metabolomic study on retinopathy of prematurity. Investigative Ophthalmology and Visual Science, 61(2), 12. [CrossRef]
39. Chong, I.G., Jun, C.H. (2005). Performance of some variable selection methods when multicollinearity is present. Chemometrics and Intelligent Laboratory Systems, 78(1), 103-112. [CrossRef]
40. Dhananjayan, K. (2015). Molecular docking study characterization of rare flavonoids at the nac-binding site of the first bromodomain of BRD4 (BRD4 BD1). Journal of Cancer Research, 2015, 1-15. [CrossRef]
41. Nabeno, M., Akahoshi, F., Kishida, H., Miyaguchi, I., Tanaka, Y., Ishii, S., Kadowaki, T. (2013). A comparative study of the binding modes of recently launched dipeptidyl peptidase IV inhibitors in the active site. Biochemical and Biophysical Research Communications, 434(2), 191-196. [CrossRef]
42. Li, D., Zhang, Y., Zhao, R. N., Fan, S., Han, J.G. (2014). Investigation on the mechanism for the binding and drug resistance of wild type and mutations of G86 residue in HIV-1 protease complexed with Darunavir by molecular dynamic simulation and free energy calculation. Journal of Molecular Modeling, 20, 2122. [CrossRef]

43. Biswas, P., Dey, D., Rahman, A., Islam, M.A., Susmi, T.F., Kaium, M.A., Hasan, M.N., Rahman, M.H., Mahmud, S., Saleh, M.A., Paul, P., Rahman, M.R., Al Saber, M., Song, H., Rahman, M.A., Kim, B. (2021). Analysis of SYK gene as a prognostic biomarker and suggested potential bioactive phytochemicals as an alternative therapeutic option for colorectal cancer: An *in-silico* pharmaco-informatics investigation. Journal of Personalized Medicine, 11, 888. [CrossRef]